

Rapid Assembly of a Library of Lipophilic Iminosugars via the Thiol–Ene Reaction Yields Promising Pharmacological Chaperones for the Treatment of Gaucher Disease

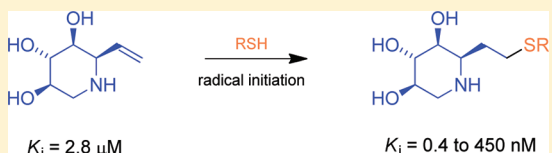
Ethan D. Goddard-Borger,[†] Michael B. Tropak,[‡] Sayuri Yonekawa,[‡] Christina Tysoe,[†] Don J. Mahuran,[‡] and Stephen G. Withers^{*†}

[†]Department of Chemistry, University of British Columbia, 2036 Main Mall, Vancouver, British Columbia, V6T 1Z1, Canada

[‡]Division of Genetics and Genome Biology, Hospital for Sick Children, 555 University Avenue, Toronto, Ontario, M5G 1X8, Canada

Supporting Information

ABSTRACT: A highly divergent route to lipophilic iminosugars that utilizes the thiol–ene reaction was developed to enable the rapid synthesis of a collection of 16 dideoxyiminoxytilols bearing various different lipophilic substituents. Enzyme kinetic analyses revealed that a number of these products are potent, low-nanomolar inhibitors of human glucocerebrosidase that stabilize the enzyme to thermal denaturation by up to 20 K. Cell based assays conducted on Gaucher disease patient derived fibroblasts demonstrated that administration of the compounds can increase lysosomal glucocerebrosidase activity levels by therapeutically relevant amounts, as much as 3.2-fold in cells homozygous for the p.N370S mutation and 1.4-fold in cells homozygous for the p.L444P mutation. Several compounds elicited this increase in enzyme activity over a relatively wide dosage range. The data assembled here illustrate how the lipophilic moiety common to many glucocerebrosidase inhibitors might be used to optimize a lead compound's ability to chaperone the protein in cellulo. The flexibility of this synthetic strategy makes it an attractive approach to the rapid optimization of glycosidase inhibitor potency and pharmacokinetic behavior.



INTRODUCTION

The lysosomal storage disorders (LSDs) are a collection of rare genetic diseases characterized by the accumulation of various metabolites within the lysosomes of the cell. These disorders are caused by mutations in genes encoding various lysosomal proteins, which leads to the impaired catabolism of the metabolite(s) in question.^{1,2} The most prevalent of the LSDs is Gaucher disease (GD), which occurs at a frequency of around 1 in 40 000 births, although it is more prevalent in some ethnic groups.³ There are three clinical types of GD, the symptoms of which have been summarized well in a review.³ Although it is worth reiterating that while all GD types may present with hepatosplenomegaly, pancytopenia, and bone abnormalities, it is only types II and III that feature neuronopathologies. These problems are ultimately caused by insufficient glucocerebrosidase (GBA) activity within the lysosomes of GD patients, which is a direct result of mutations in the encoding gene *GBA1*. GBA is a retaining β -glucosidase from glycoside hydrolase (GH) family 30 (<http://www.cazy.org>) that hydrolyzes the glycosidic bond of β -D-glucosylceramide (GC).⁴ It is the accumulation of GC that ultimately leads to the various pathologies of GD, which may in part result from perturbed intracellular calcium homeostasis in compartments such as the endoplasmic reticulum.⁵

Two therapeutic approaches are currently approved for the treatment of GD. The first and most common treatment is enzyme replacement therapy (ERT), which involves the direct administration of recombinantly expressed human GBA to supplement the patient's levels of GBA activity.³ While this is

effective in type I GD patients, this therapy is expensive and does not address the neuronopathologies of types II and III GD owing to the inability of the enzyme to cross the blood–brain barrier. The other therapy approved for GD is substrate reduction therapy (SRT).^{6,7} This approach reduces the amount of GC in a patient's lysosomes by inhibiting glucosylceramide synthase (GCS), the enzyme that creates this ubiquitous lipid. GCS inhibitors currently approved for this therapy have poor selectivity and exhibit various off-target effects,^{8,9} although more selective inhibitors and better therapeutic protocols continue to be developed.^{2,10} Regardless, one could make the case that this concept does not address the root cause of the disease state (insufficient GBA activity) and that alternative therapies that remedy this dearth of activity may have greater therapeutic potential than SRT.

There are over 200 known GD-associated missense mutations in *GBA*, and they do not appear to be localized to any one region of the enzyme.¹¹ Most of these mutations are remote to the enzyme's active site, suggesting that the majority affects GBA activity indirectly, most likely by deleteriously affecting folding of the enzyme. There is evidence to suggest that this is the case for the most common GD-associated mutation (p.N370S).^{12,13} Such mutant enzymes have difficulty obtaining and retaining their native fold within the lumen of the endoplasmic reticulum (ER), which means that a greater proportion

Received: December 2, 2011

Published: February 23, 2012

of the enzyme undergoes ER-associated degradation (ERAD) rather than reaching maturity and being trafficked to the lysosome.¹⁴ The variability in GBA activity in normal individuals is quite high,^{15,16} although type I GD patients typically have activity values that are less than 20% of the mean enzyme activity found in healthy individuals.^{15,17} If one could increase the flux of the GBA mutant to the lysosomes within the cells of a GD patient, then it might be possible to ameliorate the disease. This goal is the basis of enzyme enhancement therapy (EET), a third, as yet clinically unproven, approach to the treatment of GD.^{18–20} The EET concept proposes that small molecules could be used to bind and stabilize correctly folded mutant enzymes within the ER, thereby elevating the steady-state concentration of folded enzyme within this organelle and increasing the amount of enzyme trafficked to lysosomes. Importantly, once in the acidic and substrate-rich environment of the lysosome, the mutant enzyme should be sufficiently stable and catalytically active to perform its catabolic duties with or without the small molecule bound. Such molecules are referred to as “pharmacological chaperones” (PCs), for obvious reasons.

While it is true that a small-molecule chaperone of GBA might stabilize the enzyme through allosteric interactions alone, the vast majority of GBA chaperones identified to date do so through active site interactions.²⁰ This is not to say that occupation of the enzyme’s active site is necessarily the best way to stabilize a given GBA mutant but rather reflects the fact that high affinity, active-site-binding ligands can be rationally designed and screened for with relative ease. A typical GBA competitive inhibitor possesses two important features: (1) a D-glucopyranose-mimicking moiety to occupy the sugar binding pocket of GBA and (2) a lipophilic fragment to approximate the ceramide aglycone of the natural substrate.² This general design philosophy has led to many known glucose-like glycosidase inhibitors being modified with simple alkyl groups to generate some quite potent GBA inhibitors, some of which are capable of chaperoning the enzyme in various cell-based assays (Figure 1).

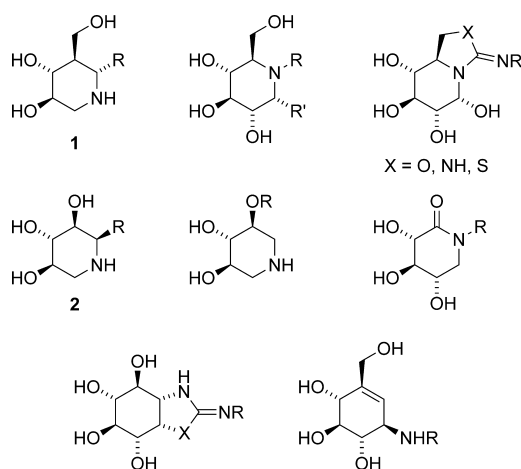


Figure 1. Structures of some GBA pharmacological chaperones.^{20–28}

While the quest for a good GBA pharmacological chaperone (PC) has seen significant effort invested into evaluating various glucose-mimicking moieties,^{20–28} considerably less attention has been devoted to exploring how the structure of the lipophilic fragment might influence the properties of the chaperone.^{29,30} For the most part, only simple straight-chain alkyl groups have been used as ceramide surrogates. This is somewhat surprising,

given that the lipophilic portion of such compounds is likely to be the most tolerant of structural variation, a significant contributor to inhibitor potency (courtesy of the hydrophobic effect), and a strong determinant of a given compound’s pharmacokinetic properties. Perhaps one reason that few have explored different lipophilic moieties at this position is that the synthesis and evaluation of such compounds as PCs using established protocols would be a laborious process. Indeed, it would be particularly arduous to prepare alkyl-chain-modified collections of the more potent glucocerebrosidase inhibitors/chaperones like the alkylated isofagomines **1** and dideoxyiminoxytols **2**, the syntheses of which involve Grignard reactions that restrict divergence and limit the chemical diversity of the lipophilic moiety. A highly divergent method for the construction of different lipophilic iminosugars based on compound **1** or **2** would provide an excellent opportunity to explore the biological consequences of this lipophilic appendage on the ability of a compound to chaperone GBA.

It was imagined that the thiol–ene reaction might be used to realize such a goal: the anti-Markovnikov addition of a given thiol to a deprotected, alkene-containing iminosugar would provide a new lipophilic iminosugar, ready for testing, in a single chemical step. In this scenario, a single sulfur atom would serve as the only apparent ligature between the sugar-mimicking and lipophilic fragments. This low profile “scar” of ligation was considered preferable to those left by other methods like, for example, the comparatively bulky triazole of an azide–alkyne cycloaddition.²⁹ If need be, the fully carbon-linked versions of the best candidates could later be synthesized and reasonably expected to possess similar affinities for GBA.

This concept was explored on the vinyl derivative of the dideoxyiminoxytols **2**: the allylamine **3** (Figure 2). This particular class of compounds was chosen because simple alkyl chain derivatives of **2** have proven to be potent and selective GBA inhibitors and competent pharmacological chaperones.²⁸

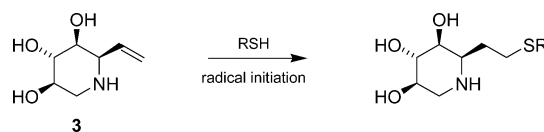
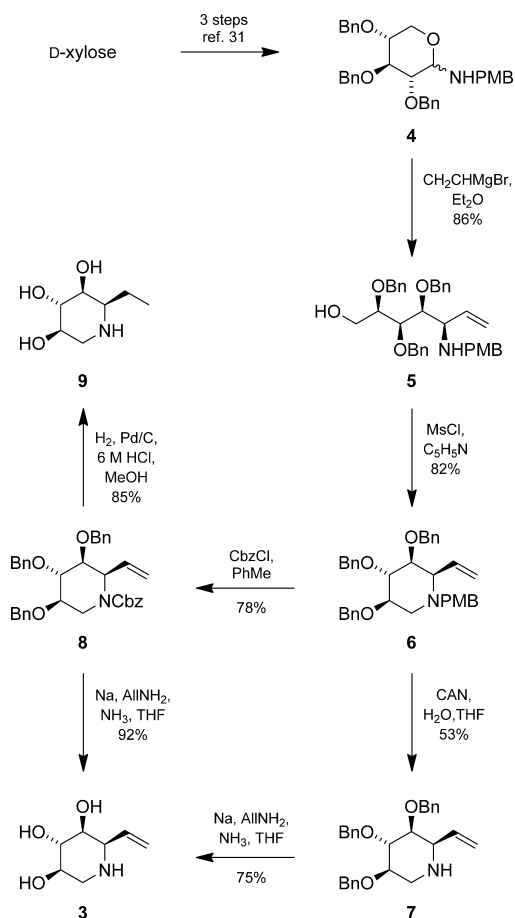


Figure 2. The thiol–ene reaction offers a highly divergent route to lipophilic iminosugars.

RESULTS AND DISCUSSION

Synthesis. The synthesis of allylamine **3** was accomplished in seven steps from D-xylose (Scheme 1). The first three steps of the sequence involved preparation of glycosylamine **4** using established protocols.³¹ This product was treated with vinylmagnesium bromide to provide the alkene **5** in good yield as the major diastereomeric product. The configuration of the new stereocenter would later be unequivocally assigned using single crystal X-ray diffraction experiments on the ultimate product, allylamine **3** (Figure 3B). Dehydrative ring closure of compound **5** was effected with methanesulfonyl chloride to provide the piperidine **6**. Attempts at global deprotection of piperidine **6** in a single step using various reducing metals in liquid ammonia were unsuccessful; in each case the *N*-(4-methoxybenzyl) group remained intact while the alkene was rapidly reduced. Thus, the *N*-(4-methoxybenzyl) moiety was first removed by the action of ceric ammonium nitrate and water to provide amine **7**, albeit in modest yield. A subsequent

Scheme 1. Synthesis of the vinyl-dideoxyiminoxylitol 3



Birch reduction of 7 provided the desired product 3, although it was necessary to perform this reaction in the presence of a vast excess of sacrificial allylamine to minimize reduction of the

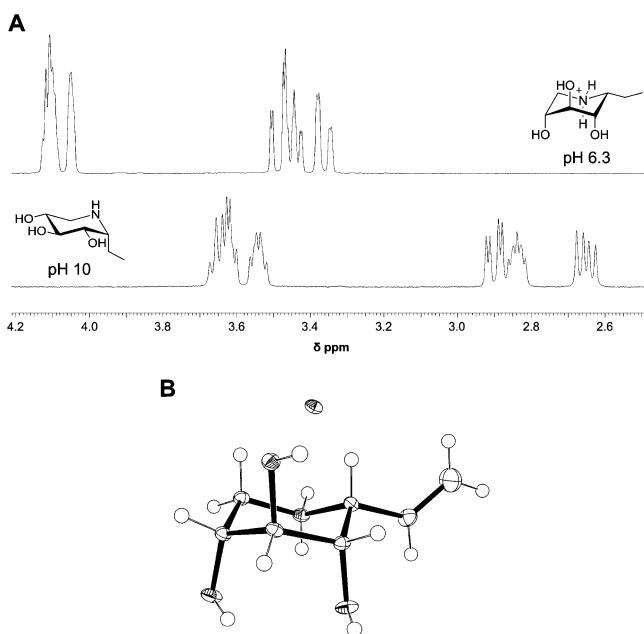


Figure 3. (A) ^1H NMR spectra of 9 reveal different conformations at high and low pH. (B) Drawing of 3-HCl with thermal ellipsoids shown at the 50% probability level.

vinyl group. Following this result, a superior deprotection strategy was devised whereby the *N*-(4-methoxybenzyl) group of 6 was initially substituted for a benzyloxycarbonyl group, by the action of benzyl chloroformate, to provide the carbamate 8. This transformation provided consistently high yields and a product that was easier to purify and more stable than the amine 7. A Birch reduction of the carbamate 8, again in the presence of excess allylamine, provided the desired product 3 in high yield. A small sample of the carbamate 8 was also subjected to hydrogenolysis to return an authentic sample of the iminosugar 9, a byproduct of the Birch reductions.

Within the literature, a number of different methods are commonly used to initiate the radical thiol–ene reaction.^{32–34} No single technique appears to work well in a general manner, and some substrate combinations simply provide poor yields under all conditions trialed. As a result, the radical thiol–ene reaction cannot really be considered a true “click” reaction, although it is certainly still a chemical transformation of great utility.^{35,36} Taking this into consideration, a number of thermal and photochemical radical initiation methods were investigated for the addition of thiols to alkene 3 (as per Figure 2). Good to moderate yields of adduct could be isolated when the reaction was promoted by AIBN in degassed methanol at reflux (Table 1), although the reaction proved to be particularly sensitive to the purity of both substrates. The thiol–ene adducts 10–25 were thereby synthesized using a range of different thiols to give products containing aromatic groups, amides, ureas, and straight, branched, and cyclic aliphatic chains of various length and size.

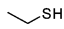
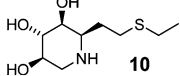
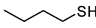
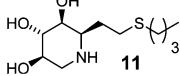

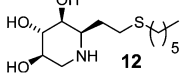
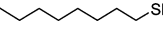
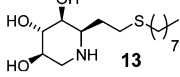
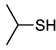
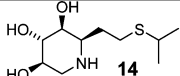
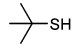
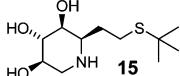
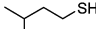
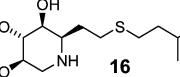
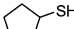
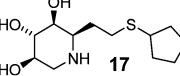
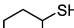
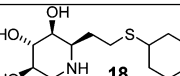
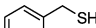
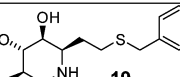
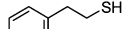
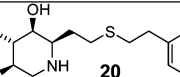
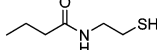
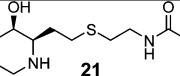
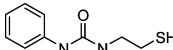
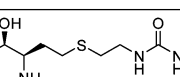
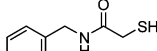
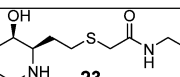
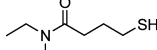
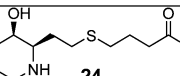
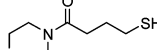
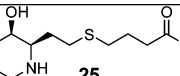
Others have noted that some dideoxyiminoxylitols appear to adopt an unusual $^2\text{C}_5$ conformation in solution, as evidenced by ^1H NMR spectroscopy, where all of the piperidine ring’s hydroxyl groups are oriented axially.²⁸ The ^1H NMR spectra of the hydrochlorides of compounds 3 and 9–25 suggest that these piperidinium ions also adopt the $^2\text{C}_5$ conformation in solution. However, at a higher pH, once deprotonated, the piperidine reverts to the $^5\text{C}_2$ conformation (Figure 3A). This pH-dependent change in conformation is consistent with the behavior of other β -hydroxypiperidines.³⁷

The $^2\text{C}_5$ conformation of the piperidinium ion was also observed in the solid state, as revealed by an X-ray diffraction experiment on a single crystal of 3-HCl (Figure 3B). This crystal structure also enabled stereochemical assignment of the chiral center that was created in the conversion of glycosylamine 4 into alkene 5 (Scheme 1).

It was imagined that this pH-dependent conformational change might be exploited to modulate the relative affinity of the iminosugars for the enzyme in the ER (pH \approx 7.0) and lysosome (pH \approx 5.5), since it seemed unlikely that the enzyme active site would accommodate a ligand with axial hydroxyl groups. To test this idea, the pK_a values of a subset of iminosugars from Table 1 were measured and the IC_{50} values of each compound against GBA determined at pH 7.0 and pH 5.5 (Table S1). Unfortunately, very little difference in inhibition of GBA was observed between these pH values, and because inhibition pH profiles are a composite of the pK_a values for free enzyme, free inhibitor, and the enzyme–inhibitor complex, it is perilous to attempt to rationalize this result.^{38–40}

Inhibition of, Specificity for, and Thermal Stability Enhancement of GBA. The inhibition constants of compounds 3 and 9–25, as well as the parent compound dideoxyiminoxylitol (2, R = H), against GBA were determined at pH 5.5 (Table 2). All of these compounds were found to

Table 1. Thiol–Ene Reactions on Alkene 3^a

Thiol	Product	Yield
		62 %
		52 %
		57 %
		47 %
		67 %
		38 %
		56 %
		63 %
		59 %
		50 %
		56 %
		43 %
		48 %
		41 %
		47 %
		39 %

^aAlkene 3 (0.1 mmol), thiol (0.5 mmol), and AIBN (20 μ mol) were refluxed in MeOH for 24 h.

inhibit GBA in a competitive manner. Every thiol–ene product had a submicromolar K_i , with one, compound 13, having a subnanomolar K_i that makes it among the tightest-binding competitive GBA inhibitors reported to date. It is worth noting that

the K_i determined for compound 12 (1.8 nM) and that previously reported for its sulfur-to-methylene homologue (2, R = *n*-nonyl; 2.2 nM)²⁸ are essentially the same. This suggests that the sulfur ligature behaves as a simple methylene surrogate on enzyme.

Several trends are apparent from the data in Table 2. First, modification of the dideoxyiminoxytilol with small groups, such as the vinyl and ethyl groups of compounds 3 and 9, does not significantly alter the parent iminosugar's affinity for GBA. However, further elaboration resulted in significant improvements in binding, as evidenced in the simplest case of compound 10, which is a 15-fold better inhibitor than the vinyl derivative 3 from which it was derived. A comparison of compounds 10–13, which all contain straight-chain aliphatic modifications, revealed that extension of this lipophilic moiety by just two methylene units improves inhibition by around an order of magnitude each time. Further, it appears that addition of a single branching methyl group can account for a 2- to 3-fold improvement in K_i , as observed for 10/14, 11/16, and 14/15. Collectively, these data illustrate in a quantitative fashion how simple modifications of the lipophilic moiety can be used to tune the potency of GBA inhibitors.

Compounds 21–25, which contain amide or urea moieties, are inherently less lipophilic than the other compounds prepared here, and yet they still retain a good affinity for GBA. It is noteworthy that compounds 22 and 23, which both contain aryl groups, were significantly better inhibitors than those amide-containing inhibitors without aryl groups.

The specificity of this collection of inhibitors for GBA over other cellular glycosidases was subsequently evaluated. Remarkably, none of the compounds inhibited human α -glucosidase, α -galactosidase, or β -galactosidase even at concentrations as high as 200 μ M, with the one exception being compound 13, which inhibited human neutral cytosolic β -glucosidase⁴¹ with an IC_{50} of 2.0 μ M. This exquisite specificity validated these chaperone candidates as target-specific.

Compounds shown to act as pharmacological chaperones for GBA (or other lysosomal enzymes for that matter) also stabilize the enzyme against thermal denaturation. Since the ability of a pharmacological chaperone to stabilize GBA is most relevant in the ER, the melting temperature of this protein was determined at pH 7.0 in the absence and presence of saturating concentrations of each inhibitor. The difference between the melting temperatures of free and inhibitor-bound GBA for each compound is presented in Table 2. An inverse linear relationship was observed between the K_i of each compound and the increase in melting temperature (Figure 4). Thus, the parent iminosugar dideoxyiminoxytilol 2, R = H, with the highest K_i (2.8 μ M) increases the melting temperature of GBA by just 3.6 K, whereas compound 13 with the lowest K_i (0.4 nM) increases the melting temperature of GBA by 20 K.

Cell-Based Assay for Pharmacological Chaperone Activity. GD patient fibroblasts homozygous for the p.N370S or p.L444P mutation were treated with each of the compounds in Table 2 to determine if any could behave as pharmacological chaperones for GBA in cellulo. The parent iminosugar dideoxyiminoxytilol 2, R = H, failed to improve GBA activity at the concentrations evaluated for either cell line. The simple vinyl and ethyl derivatives 3 and 9, all of which are hydrophilic, low micromolar inhibitors of GBA, showed minimal levels of enzyme enhancement (Figure 5). All of the other compounds were capable of increasing GBA activity at one concentration or another in fibroblasts homozygous for the

Table 2. Comparison of Kinetic, Biophysical, and Biological Parameters for the Dideoxyiminoxylitol Derivatives

subclass	compd	K_i (nM) ^a	ΔT_m (K) ^b	AC_{50} (nM) ^c		max. increase	
				p.N370S	p.L444P	p.N370S	p.L444P
parent	2,R=H	2800 ± 400	3.6	24000	44620	1.5	1.1
linear	3	2700 ± 400	3.4	1800	1700	1.4	1.3
	9	1100 ± 200	4.4	30000	7000	2.1	1.2
	10	180 ± 20	7	600	300	2.5	1.3
	11	18 ± 2	11	18	12	2.4	1.3
	12	1.8 ± 0.4	15	2.7	0.6	2.1	1.3
	13	0.4 ± 0.2	20	1.0	0.6	1.6	1.2
	14	76 ± 12	7.8	38	2.2	2.3	1.4
branched	15	29 ± 1	8.4	49	25	2.3	1.2
	16	4.4 ± 0.6	14	1.2	0.3	2.0	1.2
	17	6 ± 1	11	5.3	1.2	2.2	1.4
cyclic	18	4 ± 1	13	1.3	0.6	2.2	1.3
	19	19 ± 2	13	1.6	2.6	2.1	1.1
	20	3.0 ± 0.7	14	2.8	2.1	2.2	1.1
amide/urea	21	200 ± 20	8.2	2700	2900	2.7	1.3
	22	12 ± 2	11	90	64	2.3	1.1
	23	30 ± 2	11	190	63	2.5	1.3
	24	250 ± 20	10	800	500	2.7	1.3
	25	450 ± 50	7.6	4500	1500	3.2	1.3

^aDetermined at pH 5.5 using wild type GBA. ^bAll compounds evaluated at 100 μ M and pH 7.0 using wild type GBA. ^cConcentration at which 50% of maximum increase in intracellular GBA activity was achieved in Gaucher patient fibroblasts.

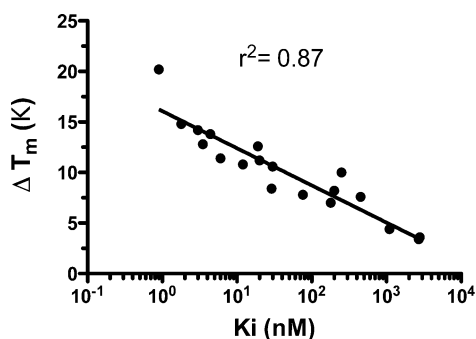


Figure 4. Relationship between K_i and ΔT_m .

p.N370S or p.L444P mutations in GBA (Figure 5, Table 2). Far greater improvements in GBA activity were observed for cells harboring the p.N370S mutation than for those with the p.L444P mutation, as has been seen with all the pharmacological chaperones of GBA evaluated to date. Interestingly, while the most lipophilic compounds with very low K_i values like 12 and 13 were able to chaperone at the lowest concentrations, it was the amide/urea-containing compounds 21–25 that elicited the most impressive improvements in GBA activity, managing a 2.3- to 3.2-fold increase in GBA activity in the p.N370S cell line and a 1.3-fold increase in the p.L444P cell line. Thus, in addition to effects that the lipophilic groups have on the inhibitory potency of the compounds these pendent groups also influence the chaperoning efficacy of drugs, possibly through effects on their bioavailability.

A subset of four compounds (13, 14, 20, and 23) were selected from each of the structural subclasses on the basis of their appended ligature (linear, branched, cyclic, and amide/urea) and were evaluated over a wider range of concentrations. This revealed that above a certain concentration for each com-

pound, the GBA activity in the cell lysate decreased (Figure 6) while, with the exception of compound 13, the activity of lysosomal β -N-acetyl hexosaminidase remained unchanged at each compound concentration. To determine if these effects were due to residual inhibitor in the cell lysate or toxicity of the compounds, the viability of GD fibroblasts grown in the presence of compounds 2 (R = H), 3, and 9–25 at three different concentrations (10, 33, and 100 μ M) was determined using a resazurin-based spectrophotometric assay. The results (Figure S1) indicate that only compounds 12 and 13 elicit a significant reduction in cell viability at the concentrations tested. Compound 12 exhibits toxicity at 100 μ M, while compound 13 is toxic at concentrations as low as 10 μ M. It is noteworthy that these two compounds are toxic at concentrations much greater than the concentrations at which they provide an enhancement in GBA activity.

The data in Table 2 also reveal a strong linear correlation between K_i and the concentration at which a half maximal increase in GBA activity (AC_{50}) is observed (Figure 7). It is of note that even though compounds 21–25 are among the least lipophilic compounds in the library and have only intermediate K_i values, they still managed to promote the greatest enhancement in GBA activity for both cell lines. It may be that these compounds strike the right balance of bioavailability and inhibitory activity to maximize enzyme enhancement. It could also be that the amide moiety is processed within the lysosome, decreasing the affinity of the resultant ligand or aiding in clearance of the inhibitor from this organelle. Certainly these amide-containing derivatives are promising candidates with great potential for further structural optimization. Another promising candidate is compound 14, which appears to provide relatively good improvements in GBA activity for both mutant cell lines over a wide range of concentrations, alluding to the possibility of a broad therapeutic dosage window. Together these compounds provide ample opportunities for further structural optimization,

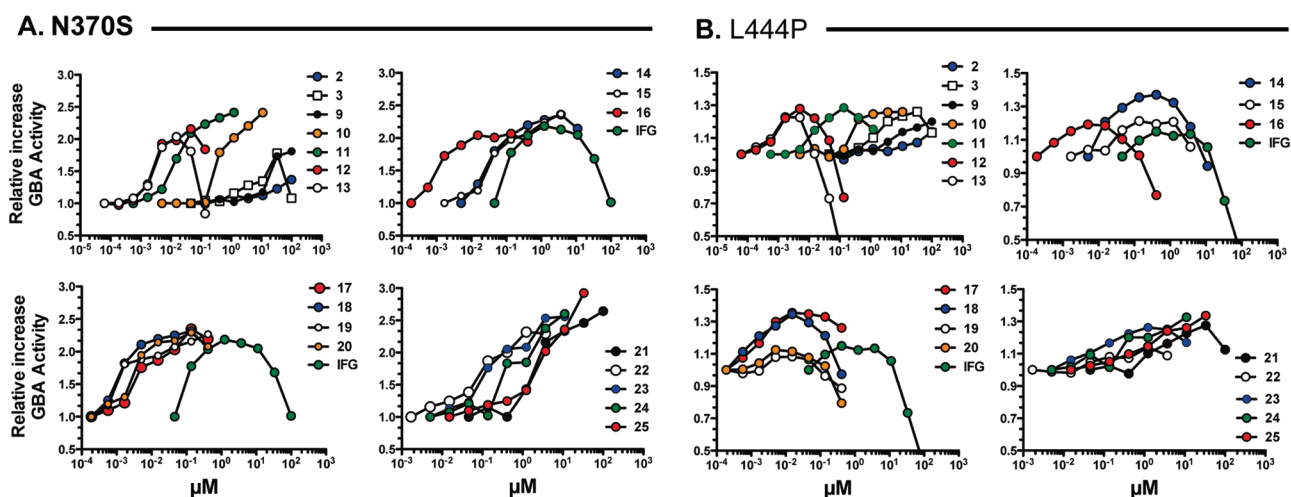


Figure 5. Increased GBA activity in compound-treated fibroblasts derived from a GD patient homozygous for (A) the p.N370S GBA mutation and (B) the p.L444P GBA mutation. Patient fibroblasts were grown in the presence of each of the compounds for 5 days. GBA activity in the lysates from treated cells was normalized to activity in untreated cells. IFG is isofagomine.

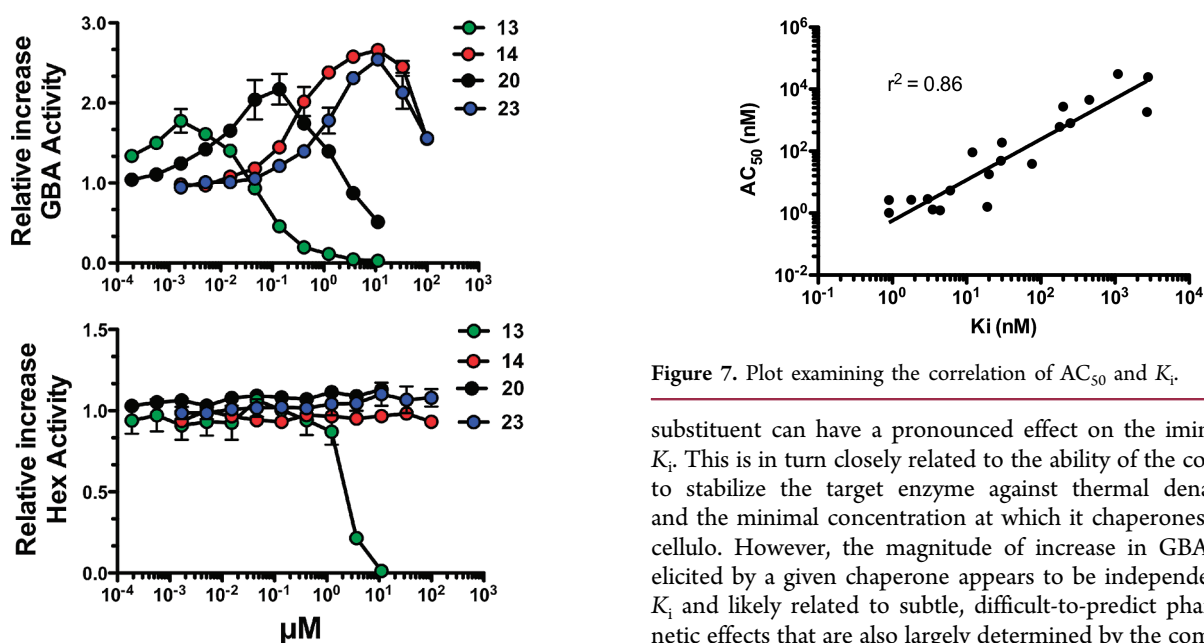


Figure 6. GBA activity in GD patient fibroblasts homozygous for the p.N370S GBA mutation when treated with representative compounds from each subclass. Patient fibroblasts were grown in the presence of each of the compounds for 5 days. GBA activity in lysates from treated cells was normalized to activity in untreated cells.

which will assist in the fine-tuning of their pharmacokinetic properties. Such second-generation compounds may provide still greater increases in GBA activity or attain similar increases at a lower dose.

CONCLUSIONS

By adoption of the thiol–ene reaction as a means to ligate various lipophilic molecules to a common iminosugar, an efficient and divergent method to prepare collections of pharmacological chaperone candidates has been developed, allowing the systematic exploration of the consequences of modifying the hydrophobic moiety therein. Results obtained with the collection of lipophilic dideoxyiminoxytilol GBA inhibitors prepared here illustrate how subtle modifications of the lipophilic

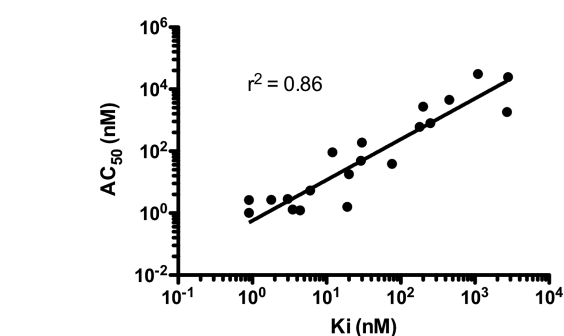


Figure 7. Plot examining the correlation of AC_{50} and K_i .

substituent can have a pronounced effect on the iminosugar's K_i . This is in turn closely related to the ability of the compound to stabilize the target enzyme against thermal denaturation and the minimal concentration at which it chaperones GBA in cellulose. However, the magnitude of increase in GBA activity elicited by a given chaperone appears to be independent of its K_i and likely related to subtle, difficult-to-predict pharmacokinetic effects that are also largely determined by the compound's lipophilic appendage. The present collection of compounds contains chaperones that possess various desirable properties, including activity at low concentrations, large therapeutic dosage windows, and very large increases in GBA activity. The methods described here will enable further structural optimization of the pharmacological chaperone leads identified in this work for the treatment of Gaucher disease. Additionally, this synthetic approach may be applicable to the identification and optimization of inhibitors of other glycosidases for use as pharmacological chaperones to treat other LSDs.

EXPERIMENTAL SECTION

General Materials and Methods. All reagents for synthesis were obtained from Sigma-Aldrich (U.S.) and were of reagent grade. All reagents were used without further purification except for the commercially obtained thiols, which were redistilled just prior to use. Thin layer chromatography (TLC) was performed on Merck silica gel 60 F₂₅₄ plates. Flash chromatography was performed with Merck silica gel 60 (230–400 mesh). ¹H and ¹³C NMR spectra (referenced using the residual solvent peak or using an internal MeOH standard in the case of ¹³C for D₂O) were recorded on a Bruker AV-300 or AV-400

instrument. High-resolution mass spectra of all compounds were obtained in the mass spectrometry laboratory of the Department of Chemistry at University of British Columbia, Canada. Pure GBA was obtained as Cerezyme from Genzyme (U.S.). Purified human cytosolic neutral β -glucosidase was kindly provided by Dr. N. Juge (Institute of Food Research, Norwich, U.K.).⁴¹ A lysosomal enriched concanavalin A fraction from human placenta was used as a source of human β -galactosidase, α -galactosidase, and α -glucosidase.⁴² Concanavalin A conjugated to agarose beads was obtained from GE Healthcare (U.S.). 2,4-Dinitrophenyl β -D-glucopyranoside was prepared according to the procedure of Sharma et al.,⁴³ while the fluorogenic enzyme substrates (4-methylumbelliferyl β -D-galactopyranoside, 4-methylumbelliferyl α -D-galactopyranoside, 4-methylumbelliferyl β -D-glucopyranoside, 4-methylumbelliferyl α -D-glucopyranoside, and 4-methylumbelliferyl *N*-acetyl- β -D-glucosaminide) were obtained commercially from Sigma-Aldrich (U.S.) or Toronto Research Chemicals (Canada). NanoOrange was obtained from Invitrogen (U.S.). Gaucher fibroblast cell lines homozygous for the p.N370S and p.L444P mutations in GBA were obtained from the cell line repositories at the Toronto Hospital for Sick Kids and the Coriell Institute for Medical Research, respectively. The purity of compounds 19–25 was determined to be >95% by analytical HPLC, while all other compounds were judged to be >95% pure by elemental microanalysis.

Enzymology. All GBA kinetics were performed at 37 °C using a buffer at pH 5.5 or pH 7.0 that contained 20 mM citric acid, 50 mM Na_2HPO_4 , 1.0 mM tetrasodium EDTA, 0.25% v/v Triton X-100, and 0.25% w/v taurocholic acid. To determine the K_i of each inhibitor for GBA, initial reaction rates were measured at three substrate concentrations for each of a range of inhibitor concentrations (typically seven concentrations bracketing the K_i ultimately determined such that $0.2K_i < [I] < 5K_i$). These data were fit to a competitive inhibition model using nonlinear regression analysis, as performed by the GraFit 5.0.13 program, to provide the K_i . Dixon and Lineweaver–Burke plots of each data set validated the use of a competitive inhibition model. For inhibitors with K_i values greater than 20 nM, this value was determined using a continuous UV spectrophotometric assay where the final GBA concentration was 4.0 nM and 2,4-dinitrophenyl β -D-glucopyranoside served as the substrate. Reactions were initiated by the addition of GBA, and the time-dependent increase in absorption at 400 nm, as determined using a Varian Cary 4000 or Varian Cary 300 UV–vis spectrophotometer, gave the initial reaction rate. This increase in absorbance was linear for all measurements over a period of 3 min. For inhibitors with K_i values less than 20 nM, this value was determined using a discontinuous fluorimetric assay where the final GBA concentration was 10 pM and 4-methylumbelliferyl β -D-glucopyranoside served as the substrate. Reactions were initiated by the addition of GBA, and after 4, 10, and 15 min, 150 μL aliquots of the reaction mixture were removed and diluted into a cuvette containing 450 μL of glycine buffer (1.0 M, pH 10.8). The fluorescence of each sample ($\lambda_{\text{ex}} = 365$ nm, $\lambda_{\text{em}} = 460$ nm) was determined using a Varian Cary Eclipse fluorimeter. The three time points were fit by linear regression to provide the initial reaction rate. In each case, an excellent linear fit was obtained over this 15 min interval. The inhibitory activities of compounds against selected human lysosomal enzymes (α -glucosidase, α -galactosidase, and β -galactosidase) were evaluated at a single, high concentration of 200 μM , in triplicate. All reactions were performed using 100 mM citrate–phosphate buffer at pH 4.5 supplemented with 0.025% w/v human serum albumin. The activities of human lysosomal α -glucosidase, α -galactosidase, and β -galactosidase in a lysosomal enzyme enriched ConA-bound fraction from human placenta were monitored using an equal volume of the fluorogenic substrates [4-methylumbelliferyl α -D-glucopyranoside (3.0 mM), 4-methylumbelliferyl α -D-galactopyranoside (1.0 mM), and 4-methylumbelliferyl β -D-galactopyranoside (0.5 mM), respectively] at 37 °C. All reactions were terminated by the addition of a 4-fold excess of 100 mM 2-amino-2-methylpropanol (MAP), and fluorescence was measured using a Molecular Devices M2 fluorimeter ($\lambda_{\text{ex}} = 365$ nm, $\lambda_{\text{em}} = 460$ nm). Inhibitory activities against purified cytosolic neutral human β -glucosidase were determined by incubating a 3-fold dilution series of the compound in the presence of the enzyme for 15 min at room

temperature, followed by the addition of an equal volume of substrate (10 mM 4-methylumbelliferyl β -D-glucopyranoside) in 100 mM citrate–phosphate buffer at pH 7.0. Each mixture was incubated at 37 °C for 30 min. The reaction was terminated by the addition of a 4-fold excess of 100 mM MAP and the fluorescence determined as described above. IC_{50} values were deduced by nonlinear fitting of the data to the appropriate model using Prism Graphpad, version 5.2.

Differential Scanning Fluorimetry. The melting temperatures of human GBA (1 μg) in the presence of compounds 2 ($R = \text{H}$), 3, and 9–25 (200 μM) were determined by scanning differential fluorimetry, using NanoOrange ($1/100$ dilution as per the manufacturer's protocol) as the fluorescent reporter, in accordance with established protocols.⁴⁴

Cell-Based Assay for GBA Chaperone Activity. Patient fibroblasts homozygous for the p.N370S mutation or p.L444P mutation were grown in 96-well tissue culture plates (10–20000 cells/well) in α -MEM medium supplemented with 10% v/v fetal calf serum at 37 °C in a CO_2 humidified incubator. Chaperone efficiencies of the compounds were evaluated by preparing a series of 3-fold dilutions starting at 10 mM in water. Compounds were directly added to the media at a $1/100$ dilution. Following incubation of the cells for 5 days in the compound-supplemented medium, lysates in 100 mM citrate–phosphate buffer at pH 5.5 containing 0.4% v/v Triton X-100 and 0.2% w/v taurocholic acid were prepared as described.⁴⁵ GBA activity was measured using 10 mM 4-methylumbelliferyl β -D-glucopyranoside, and for compound treated cells, this value was normalized against the GBA activity measured in mock-treated control cells ($n = 3$). Similar activity measurements were also performed for lysosomal hexosaminidase (Hex) using 3.2 mM 4-methylumbelliferyl *N*-acetyl- β -D-glucosaminide as the substrate.

Thiol–Ene Reaction Protocol. A solution of AIBN (3.3 mg, 20 μmol) in degassed MeOH (1.0 mL) was added dropwise over 8 h to a solution of thiol (0.50 mmol) and alkene 3 (16 mg, 0.10 mmol) in degassed MeOH (2.0 mL) refluxing under an atmosphere of N_2 . The solution was refluxed for a further 16 h, concentrated to dryness, and then subjected to flash chromatography. The product was dissolved in HCl (2.0 mL, 0.1 M) and the solution concentrated to dryness. The residue was dissolved in H_2O and passed through a Waters tC18 Sep-Pak (2 g, $\text{H}_2\text{O}/\text{MeOH}$, 1:0 to 1:4). Fractions containing product were combined and lyophilized.

■ ASSOCIATED CONTENT

Supporting Information

pK_a and IC_{50} data for selected iminosugars, solution and refinement data for the single crystal X-ray diffraction experiment, cell viability assay data, experimental and characterization data, ^1H and ^{13}C NMR spectra for all novel compounds, and crystallographic information file in txt format. This material is available free of charge via the Internet at <http://pubs.acs.org>.

■ AUTHOR INFORMATION

Corresponding Author

*Telephone: (604) 822-3402. E-mail: witthers@chem.ubc.ca.

Notes

The authors declare the following competing financial interest(s): Patent protection has been sought by the Hospital for Sick Children (Toronto) and the University of British Columbia.

■ ACKNOWLEDGMENTS

This work was funded by the Canadian Institutes of Health Research through a TEAM grant. E.D.G.-B thanks the Canadian Institutes of Health Research for a postdoctoral fellowship. S.G.W. acknowledges support from the Canada Research Chairs Program, the Canadian Foundation for Innovation, and the B.C. Knowledge Development Fund. Jennifer Dhammi is acknowledged for assistance in the laboratory.

■ ABBREVIATIONS USED

LSD, lysosomal storage disorder; GD, Gaucher disease; GBA, glucosidase, beta, acid (glucocerebrosidase); GH, glycoside hydrolase (glycosidase); GC, β -D-glucopyranosyl ceramide; ERT, enzyme replacement therapy; SRT, substrate reduction therapy; GCS, glucosylceramide synthase; ER, endoplasmic reticulum; ERAD, endoplasmic reticulum associated degradation; EET, enzyme enhancement therapy; PC, pharmacological chaperone; IFG, isofagomine.

■ REFERENCES

- (1) Futerman, A. H.; van Meer, G. The cell biology of lysosomal storage disorders. *Nat. Rev. Mol. Cell Biol.* **2004**, *5*, 554–565.
- (2) Wenekes, T.; van den Berg, R. J.; Boot, R. G.; van der Marel, G. A.; Overkleeft, H. S.; Aerts, J. M. Glycosphingolipids: nature, function, and pharmacological modulation. *Angew. Chem., Int. Ed. Engl.* **2009**, *48*, 8848–8869.
- (3) Grabowski, G. A. Phenotype, diagnosis, and treatment of Gaucher's disease. *Lancet* **2008**, *372*, 1263–1271.
- (4) Vocadlo, D. J.; Davies, G. J. Mechanistic insights into glycosidase chemistry. *Curr. Opin. Chem. Biol.* **2008**, *12*, 539–555.
- (5) Vitner, E. B.; Platt, F. M.; Futerman, A. H. Common and uncommon pathogenic cascades in lysosomal storage diseases. *J. Biol. Chem.* **2010**, *285*, 20423–20427.
- (6) Pastores, G. M.; Giraldo, P.; Chérin, P.; Mehta, A. Goal-oriented therapy with miglustat in Gaucher disease. *Curr. Med. Res. Opin.* **2009**, *25*, 23–37.
- (7) Butters, T. D.; Dwek, R. A.; Platt, F. M. Imino sugar inhibitors for treating the lysosomal glycosphingolipidoses. *Glycobiology* **2005**, *15*, 43R–52R.
- (8) Belmatoug, N.; Burlina, A.; Giraldo, P.; Hendriks, C. J.; Kuter, D. J.; Mengel, E.; Pastores, G. M. Gastrointestinal disturbances and their management in miglustat-treated patients. *J. Inherited Metab. Dis.* **2011**, *34*, 991–1001.
- (9) Porto, C.; Cardone, M.; Fontana, F.; Rossi, B.; Tuzzi, M. R.; Tarallo, A.; Barone, M. V.; Andria, G.; Parenti, G. The pharmacological chaperone N-butyldeoxyjirimycin enhances enzyme replacement therapy in Pompe disease fibroblasts. *Mol. Ther.* **2009**, *17*, 964–971.
- (10) Marshall, J.; McEachern, K. A.; Chuang, W. L.; Hutto, E.; Siegel, C. S.; Shayman, J. A.; Grabowski, G. A.; Scheule, R. K.; Copeland, D. P.; Cheng, S. H. Improved management of lysosomal glucosylceramide levels in a mouse model of type 1 Gaucher disease using enzyme and substrate reduction therapy. *J. Inherited Metab. Dis.* **2010**, *33*, 281–289.
- (11) Hruska, K. S.; LaMarca, M. E.; Scott, C. R.; Sidransky, E. Gaucher disease: mutation and polymorphism spectrum in the glucocerebrosidase gene (GBA). *Hum. Mutat.* **2008**, *29*, 567–583.
- (12) Steet, R. A.; Chung, S.; Wustman, B.; Powe, A.; Do, H.; Kornfeld, S. A. The iminosugar isofagomine increases the activity of N370S mutant acid beta-glucosidase in Gaucher fibroblasts by several mechanisms. *Proc. Natl. Acad. Sci. U.S.A.* **2006**, *103*, 13813–13818.
- (13) Wei, R. R.; Hughes, H.; Boucher, S.; Bird, J. J.; Guziewicz, N.; van Patten, S. M.; Qiu, H.; Pan, C. Q.; Edmunds, T. X-ray and biochemical analysis of N370S mutant human acid β -glucosidase. *J. Biol. Chem.* **2011**, *286*, 299–308.
- (14) Ron, I.; Horowitz, M. ER retention and degradation as the molecular basis underlying Gaucher disease heterogeneity. *Hum. Mol. Genet.* **2005**, *14*, 2387–2398.
- (15) Legini, E.; Orsini, J. J.; Hung, C.; Martin, M.; Showers, A.; Scarpa, M.; Zhang, X. K.; Keutzer, J.; Muhl, A.; Bodamer, O. A. Analysis of glucocerebrosidase activity in dry blood spots using tandem mass spectrometry. *Clin. Chim. Acta* **2011**, *412*, 343–346.
- (16) Li, Y.; Scott, C. R.; Chamoles, N. A.; Ghavami, A.; Pinto, B. M.; Turecek, F.; Gelb, M. H. Direct multiplex assay of lysosomal enzymes in dried blood spots for newborn screening. *Clin. Chem.* **2004**, *50*, 1785–1796.
- (17) Grabowski, G. A.; Goldblatt, J.; Dinur, T.; Kruse, J.; Svennerholm, L.; Gatt, S.; Desnick, R. J. Genetic heterogeneity in Gaucher disease: physicochemical and immunologic studies of the residual enzyme in cultured fibroblasts from non-neuronopathic and neuronopathic patients. *Am. J. Med. Genet.* **1985**, *21*, 529–549.
- (18) Parenti, G. Treating lysosomal storage diseases with pharmacological chaperones: from concept to clinics. *EMBO Mol. Med.* **2009**, *1*, 268–279.
- (19) Valenzano, K. J.; Khanna, R.; Powe, A. C. Jr.; Boyd, R.; Lee, G.; Flanagan, J. J.; Benjamin, E. R. Identification and characterization of pharmacological chaperones to correct enzyme deficiencies in lysosomal storage disorders. *Assay Drug Dev. Technol.* **2011**, *9*, 213–235.
- (20) Benito, J. M.; Garcia Fernandez, J. M.; Mellet, C. O. Pharmacological chaperone therapy for Gaucher disease: a patent review. *Expert Opin. Ther. Pat.* **2011**, *21*, 885–903.
- (21) Butters, T. D. Gaucher disease. *Curr. Opin. Chem. Biol.* **2007**, *11*, 412–418.
- (22) Chang, H.-H.; Asano, N.; Ishii, S.; Ichikawa, Y.; Fan, J.-Q. Hydrophilic iminosugar active-site-specific chaperones increase residual glucocerebrosidase activity in fibroblasts from Gaucher patients. *FEBS J.* **2006**, *273*, 4082–4092.
- (23) Luan, Z.; Higaki, K.; Aguilar-Moncayo, M.; Li, L.; Ninomiya, H.; Nanba, E.; Ohno, K.; García-Moreno, M. L.; Ortiz Mellet, C.; García Fernández, J. M.; Suzuki, Y. A fluorescent sp²-iminosugar with pharmacological chaperone activity for Gaucher disease: synthesis and intracellular distribution studies. *ChemBioChem* **2010**, *11*, 2453–2464.
- (24) Wang, G.-N.; Reinkensmeier, G.; Zhang, S.-W.; Zhou, J.; Zhang, L.-R.; Zhang, L.-H.; Butters, T. D.; Ye, X.-S. Rational design and synthesis of highly potent pharmacological chaperones for treatment of N370S mutant Gaucher disease. *J. Med. Chem.* **2009**, *52*, 3146–3149.
- (25) Zhu, X.; Sheth, K. A.; Li, S.; Chang, H.-H.; Fan, J.-Q. Rational design and synthesis of highly potent β -glucocerebrosidase inhibitors. *Angew. Chem., Int. Ed.* **2005**, *44*, 7450–7453.
- (26) Trapero, A.; Alfonso, I.; Butters, T. D.; Llebaria, A. Polyhydroxylated bicyclic isoureas and guanidines are potent glucocerebrosidase inhibitors and nanomolar enzyme activity enhancers in Gaucher cells. *J. Am. Chem. Soc.* **2011**, *133*, 5474–5484.
- (27) Oulaïdi, F.; Front-Deschamps, S.; Gallienne, E.; Lesellier, E.; Ikeda, K.; Asano, N.; Compain, P.; Martin, O. R. Second-generation iminoxylitol-based pharmacological chaperones for the treatment of Gaucher disease. *ChemMedChem* **2011**, *6*, 353–361.
- (28) Compain, P.; Martin, O. R.; Boucheron, C.; Godin, G.; Yu, L.; Ikeda, K.; Asano, N. Design and synthesis of highly potent and selective pharmacological chaperones for the treatment of Gaucher's disease. *ChemBioChem* **2006**, *7*, 1356–1359.
- (29) Diot, J. D.; Moreno, I. G.; Twigg, G.; Mellet, C. O.; Haupt, K.; Butters, T. D.; Kovensky, J.; Gouin, S. G. Amphiphilic 1-deoxyjirimycin derivatives through click strategies for chemical chaperoning in N370S Gaucher cells. *J. Org. Chem.* **2011**, *76*, 7757–7768.
- (30) Ardes-Guisot, N.; Alonzi, D. S.; Reinkensmeier, G.; Butters, T. D.; Norez, C.; Becq, F.; Shimada, Y.; Nakagawa, S.; Kato, A.; Blériot, Y.; Sollogoub, M.; Vauzeilles, B. Selection of the biological activity of DNJ neoglycoconjugates through click length variation of the side chain. *Org. Biomol. Chem.* **2011**, *9*, 5373–5388.
- (31) Wenekes, T.; van den Berg, R. J. B. H. N.; Boltje, T. J.; Donker-Koopman, W. E.; Kuijper, B.; van der Marel, G. A.; Strijland, A.; Verhagen, C. P.; Aerts, J. M. F. G.; Overkleeft, H. S. Synthesis and evaluation of lipophilic aza-C-glycosides as inhibitors of glucosylceramide metabolism. *Eur. J. Org. Chem.* **2010**, 1258–1283.
- (32) Uygun, M.; Tasdelen, M. A.; Yagci, Y. Influence of type of initiation on thiol–ene “click” chemistry. *Macromol. Chem. Phys.* **2010**, *211*, 103–110.
- (33) Griesbaum, K. Problems and possibilities of the free-radical addition of thiols to unsaturated compounds. *Angew. Chem., Int. Ed. Engl.* **1970**, *9*, 273–287.
- (34) Wittrock, S.; Becker, Y.; H., K. Synthetic vaccines of tumor-associated glycopeptide antigens by immune-compatible thioether

linkage to bovine serum albumin. *Angew. Chem., Int. Ed.* **2007**, *46*, 5226–5230.

(35) Fiore, M.; Marra, A.; Dondoni, A. Photoinduced thiol–ene coupling as a click ligation tool for thiodisaccharide synthesis. *J. Org. Chem.* **2009**, *74*, 4422–4425.

(36) Koo, S. P. S.; Stamenovic, M. M.; Prasath, R. A.; Inglis, A. J.; Du Prez, F. E.; Barner-Kowollik, C.; van Camp, W.; Junkers, T. Limitations of radical thiol–ene reactions for polymer–polymer conjugation. *J. Polym. Sci., Part A: Polym. Chem.* **2010**, *48*, 1699–1713.

(37) Asensio, J. L.; Cañada, F. J.; García-Herrero, A.; Murillo, M. T.; Fernández-Mayoralas, A.; Johns, B. A.; Kozak, J.; Zhu, Z.; Johnson, C. R.; Jiménez-Barbero, J. Conformational behavior of aza-C-glycosides: experimental demonstration of the relative role of the exo-anomeric effect and 1,3-type interactions in controlling the conformation of regular glycosides. *J. Am. Chem. Soc.* **1999**, *121*, 11318–11329.

(38) van Bueren, A. L.; Popat, S. D.; Lin, C.-H.; Davies, G. J. Structural and thermodynamic analyses of α -L-fucosidase inhibitors. *ChemBioChem* **2010**, *11*, 1971–1974.

(39) Gloster, T. M.; Meloncelli, P. J.; Stick, R. V.; Zechel, D.; Vasella, A.; Davies, G. J. Glycosidase inhibition: an assessment of the binding of 18 putative transition-state mimics. *J. Am. Chem. Soc.* **2007**, *129*, 2345–2354.

(40) Knowles, J. R. The intrinsic pKa-values of functional groups in enzymes: improper deductions from the pH-dependence of steady-state parameters. *Crit. Rev. Biochem.* **1976**, *4*, 165–173.

(41) Tribolo, S.; Berrin, J. G.; Kroon, P. A.; Czjzek, M.; Juge, N. The crystal structure of human cytosolic β -glucosidase unravels the substrate aglycone specificity of a family 1 glycoside hydrolase. *J. Mol. Biol.* **2007**, *370*, 964–975.

(42) Mahuran, D.; Lowden, J. A. The subunit and polypeptide structure of hexosaminidases from human placenta. *Can. J. Biochem.* **1980**, *58*, 287–294.

(43) Sharma, S. K.; Corrales, G.; Penadés, S. Single step stereoselective synthesis of unprotected 2,4-dinitrophenyl glycosides. *Tetrahedron Lett.* **1995**, *36*, 5627–5630.

(44) Kornhaber, G. J.; Tropak, M. B.; Maegawa, G. H.; Tuske, S. J.; Coales, S. J.; Mahuran, D. J.; Hamuro, Y. Isofagomine induced stabilization of glucocerebrosidase. *ChemBioChem* **2008**, *9*, 2643–2649.

(45) Hill, T.; Tropak, M. B.; Mahuran, D.; Withers, S. G. Synthesis, kinetic evaluation and cell-based analysis of C-alkylated isofagomines as chaperones of β -glucocerebrosidase. *ChemBioChem* **2011**, *12*, 2151–2154.